

Accepted Manuscript

A novel CuO NPs/AgZSM-5 zeolite composite adsorbent: Synthesis, identification and its application for the removal of sulfur mustard agent simulate

Meysam Sadeghi, Sina Yekta, Daryoush Mirzaei



PII: S0925-8388(18)31109-5

DOI: [10.1016/j.jallcom.2018.03.239](https://doi.org/10.1016/j.jallcom.2018.03.239)

Reference: JALCOM 45469

To appear in: *Journal of Alloys and Compounds*

Received Date: 11 December 2017

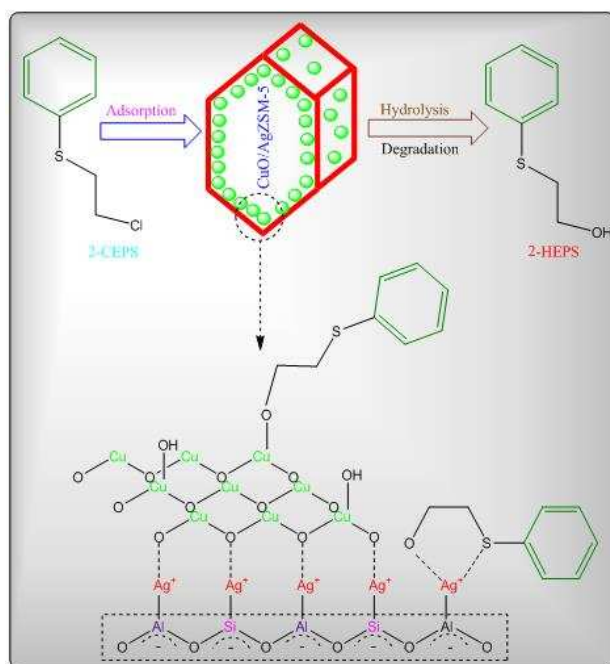
Revised Date: 17 March 2018

Accepted Date: 19 March 2018

Please cite this article as: M. Sadeghi, S. Yekta, D. Mirzaei, A novel CuO NPs/AgZSM-5 zeolite composite adsorbent: Synthesis, identification and its application for the removal of sulfur mustard agent simulate, *Journal of Alloys and Compounds* (2018), doi: 10.1016/j.jallcom.2018.03.239.

This is a PDF file of an unedited manuscript that has been accepted for publication. As a service to our customers we are providing this early version of the manuscript. The manuscript will undergo copyediting, typesetting, and review of the resulting proof before it is published in its final form. Please note that during the production process errors may be discovered which could affect the content, and all legal disclaimers that apply to the journal pertain.

Graphical abstract



A novel CuO NPs/AgZSM-5 zeolite composite adsorbent: synthesis, identification and its application for the removal of sulfur mustard agent simulate

Meysam Sadeghi^a, Sina Yekta^{b*}, Daryoush Mirzaei^a

^aDepartment of Chemistry, Lorestan University, Khorramabad, Iran

^bDepartment of Chemistry, Payame Noor University, P.O. BOX. 4693179573, Ramsar, Iran

*E-mail: sina.yekta.chem@gmail.com

Tel: +98-09039841109

Fax: +98-01155254021

Orcid ID: <https://orcid.org/0000-0001-5249-0855>

Abstract

In this investigation, the parent NaZSM-5 zeolite has been successfully fabricated by the hydrothermal route and then to enhance the catalytic performance of this zeolite, silver ions (Ag^+) and copper oxide nanoparticles (CuO NPs) were loaded in its structure through the ion exchange and impregnation methods to attain the novel CuO NPs/AgZSM-5 zeolite composite adsorbent. The parent and modified samples were comprehensively analyzed and identified by using the FESEM-EDX, TEM, XRD, and FTIR techniques. This is the first time that the CuO NPs/AgZSM-5 (containing 3.4 wt.% Ag and 12.6 wt.% CuO) has been utilized for the removal (adsorption and degradation) of 2-chloroethyl phenyl sulfide (2-CEPS) as a toxic sulfur mustard agent simulate, and its applicability was proved according to the GC-FID, GC-MS, and FTIR results. Moreover, the consequences of several experimental factors such as contact time, initial concentration, adsorbent dose, and adsorbent type on the removal efficiency of 2-CEPS were also surveyed. The GC-FID analysis data confirmed that the maximum removal yield of 2-CEPS was 100%. Besides, the parameters of contact time (120 min), initial concentration (25 mg/L), and adsorbent dose (0.3 g) were perused and optimized for the subsequent reaction. The reaction kinetic status was also studied employing first order model. The quantities of the half-life ($t_{1/2}$) and rate constant (k) were indicated as 26.25 min and 0.0264 min^{-1} , respectively. The product obtained from the degradation and hydrolysis reaction between the 2-CEPS and CuO NPs/AgZSM-5 was 2-hydroxy ethyl phenyl sulfide (2-HEPS) which is substantially less toxic than original pesticide.

Keywords: CuO NPs/AgZSM-5, 2-CEPS, removal, adsorption, degradation.

1. Introduction

The major perspective of science and scientific advances should be providing solutions for numerous complex problems with which human beings have been struggling for long time now. But,

unfortunately one of the most hideous facts of these scientific developments is to turning them to the opposite side and against humanity and moral values which is due to embracing more domination and power on other parties. Another serious concern which has been obsessing minds toward itself is what happens if these opposite scientific advances become available for terrorist groups or organizations around the world. In this matter, the Chemical Warfare Agents (CWA) can be named as one of the malicious outcomes of those mentioned shameful and dark corners of scientific developments. These agents were fabricated and designed to negatively impact the crowd by any route of exposure and to be effective even at slight doses. The CWAs are intended to be used in military aspects for mass killing purposes, or incapacitate people owing to their highly disastrous physiological effects [1, 2]. Also, their release impacts the environment and contaminates the ground waters. Thus, it is of great significance to find applicable approaches for their destruction and disposal. The sulfur mustard is recognized as one of the main sorts of these chemical weapons. Sulfur mustard, bis-(2-chloroethyl) sulfide, also known as HD, S-mustard, HS, etc smells as garlic or mustard. But on the other hand, its disabling vapor concentration is likely to have trivial odor that one will not be able to sense until the first aftereffect appears. Further, it is tasteless and colorless, which makes it extremely dangerous since its detection become considerably impossible by the senses. Besides, HD has been known as a human carcinogen which obligates harmful consequences to the body by interfering chemical reactions with cellular constituents. The nicotinamide adenine dinucleotide (NAD) depletion, prevention of mitosis, reduced tissue respiration and eventually death are the results of such implied biochemical reactions [3-5]. It is also notable that World War I, Syria, and Iran-Iraq war are some irrefutable examples when the HD agent released for calamitous massacre. The 2-chloroethyl phenyl sulfide (2-CEPS) is a known simulate of sulfur mustard which has been frequently used in numerous researches as the less toxic sort of this chemical agent [6]. Considering a high yield adsorption-degradation, it is essential to synthesis an applicable adsorbent. ZSM-5 (MFI-type zeolite), first introduced by Argauer and Landolt in 1972 [7], is a zeolite comprising three-dimensional channels designated by 10-membered rings with average pore size of 6Å. ZSM-5 offers particular properties such as unexampled channel structure, shape selectivity, thermal stability, acidity which make them superior to be utilized as catalyst and sorbent in several fields like fine chemical production, liquid and gas separation, and petrochemical processing [8,9]. Recently growing attention has been devoted to synthesis procedure, characteristics and numerous applications of ZSM-5 zeolites. Meanwhile, different templates have been defined for the synthesis process of ZSM-5 zeolites, namely tetrapropylamine bromide. In this regard, the substance used as template, the quality of the reagents, and the gel composition, are some of major parameters that may affect the physicochemical characteristics of ZSM-5 zeolites. Thereupon, it is of great significance to consider and use an appropriate template for the synthesis of ZSM-5 [10-12]. In fact, MFI-type zeolite with those above mentioned 10-membered oxygen rings and equal pore structure is effectively able to display a host behavior and entrap the guest molecules into the micropores. On the other hand, considering the

unprecedented features of the combination of microporous solid materials with nanoparticles including high surface area along with the open framework and also the well-designated pore size, the microporous solid materials loaded with nanoparticles have recently attracted significant attention. The semiconductor nanoparticles are good example of this implied combination. In this matter, to functionalize both surface area and microporous internal surface of the microporous materials and their subsequent use as host materials, an appropriate modification process should be implemented [13,14]. Furthermore, in recent years, the perception of wide potential and applicability of metal oxide nanoparticles has opened a new window toward synthesis and use of these nanomaterials for multipurpose use in different scientific fields. The characteristics of nanomaterials are highly related to the morphology, size and particular surface area of the synthesized nanomaterials [15]. Due to having specific physical and chemical properties differing from bulk, they have been greatly employed in several fields for instance optoelectronics, sensing, solar cells and catalysis. TiO_2 [16, 17], CaO [18], Y_2O_3 nanoparticles [19], MgO [5,20], ZnO [21], and Fe_3O_4 [22] etc are some examples of transition metal oxides which have been utilized in numerous scientific researches. Copper (II) oxide (CuO) or known as cupric oxide is also one of the most applying metal oxides which have been used for many applications in various fields. Besides, it represents a superior monoclinic tenorite structure and also shows p-type semiconductor behavior with an indirect band gap of 1.21-1.51 eV [23, 24]. The semiconductor materials have been the center of attentions regarding to their substantial role in electronic and optoelectronic devices. They have been considerably used in gas sensors [25], magnetic storage systems [26], electro chemical cell [27], field emitters [28], nano fluid [29], super conductors [30], and catalysts [31] etc. Moreover, CuO has been extensively employed as an environmental catalyst for the degradation of environmental pollutants [32, 33]. To synthesis the CuO nanoparticles, several methods can be considered including sol-gel [34], precipitation [35], thermal decomposition [36], and alcothermal method [37]. Apart from what explained about CuO , Ag^+ was also applied because of its unique catalytic characteristics [38, 39]. From this combination basis, in our previous studies, two different composite adsorbents of Pb-MCM-41/ZnNiO_2 [40] and $\text{NiO NPs/Ag-clinoptilolite}$ [41] were synthesized and introduced for the first time for the adsorption and degradation of CWAs. In the current study, to develop a much superior adsorbent for such lethal chemical warfare with lesser time of reaction and applicability for higher concentrations of 2-CEPS compared with those previously mentioned ones, the CuO NPs/AgZSM-5 as a novel zeolite composite adsorbent synthesized via the impregnation method is represented and punctually discussed.

2. Experimental

The chemical reagents were all of analytical grade and utilized as received with no extra purification process. Sodium hydroxide pellets (NaOH), sodium aluminate (NaAlO_2), silicic acid (H_2SiO_3), 2-chloroethyl phenyl sulfide (2-CEPS), n-octane, n-decane, copper nitrate trihydrate ($\text{Cu}(\text{NO}_3)_2 \cdot 3\text{H}_2\text{O}$),

silver nitrate (AgNO_3), and hydrochloric acid (HCl) were all purchased from Sigma-Aldrich chemical company. Further, the deionized water (D.W) was employed throughout the research.

2.1. Instrumentation

The functional groups, morphology, crystalline structure, elemental composition, and structure features are known as some physicochemical characteristics of the understudy samples which have been investigated via several analytical techniques. To observe the morphology and elemental composition analysis of the samples, a Field emission scanning electron microscopy-energy dispersive X-ray spectroscopy (FESEM-EDX) on a MIRA3 TESCAN was operated. The shape and size of the samples were indicated by transmission electron microscopy (TEM) on an EM10C microscope functioning at an advancing voltage of 100 Kv. Moreover, using a Philips X'pert Pro diffractometer equipped with $\text{CoK}\alpha$ radiation at wavelength of 1.54056 \AA (30 mA and 40 kV) at room temperature, the powder X-ray diffraction (XRD) patterns were obtained. In this regard, the corresponded data were gathered over in the 2θ range of 4° - 80° with a scanning speed of 2° min^{-1} . The Fourier transform infrared (FTIR) were acquired on a Shimadzu system FTIR 160 spectrophotometer in the wavelength scope of 400 to 4000 cm^{-1} using KBr disks the technique. Besides, To monitor the hydrolysis reactions of the 2-chloroethyl phenyl sulfide (2-CEPS), a Varian Star 3400CX series gas chromatograph associated with flame ionization detector (GC-FID) and an OV-101CWHP 80/100 silica capillary column ($30 \text{ m} \times 0.25 \text{ mm}$ inner diameter (i.d.), $0.25 \text{ }\mu\text{m}$ film thickness) was operated and the related results were recorded. The gained products were investigated by a HP-Agilent gas chromatograph-mass spectrometer fitted with a fused-silica capillary column (DB 1701, $30 \text{ m} \times 0.25 \text{ mm}$ inner diameter (i.d.), $0.25 \text{ }\mu\text{m}$ film thickness). Also, the GC utilized under the conditions of: the column temperature was first set at 60°C for 5min and then adjusted at $20^\circ\text{C min}^{-1}$ to 200°C to reach the ultimate temperature at which was held for 13 min. Plus, the injector, MS quad and source temperatures were programmed at 60°C , 200°C and 230°C , respectively. Helium (99.999% purity) with the flow rate of 1 mL min^{-1} was applied as the carrier gas.

2.2. Synthesis of NaZSM-5

To synthesize the NaZSM-5 zeolite, the hydrothermal method was applied as a typical procedure. At First, the values of 50 mmol sodium hydroxide pellets (NaOH) and 6 mmol sodium aluminate (NaAlO_2) were added and subsequently dissolved in the deionized water (D.W) and then transferred to a polypropylene bottle. Next, this mixture was undergone agitation on a shaker for overnight. After the mentioned mixture was appropriately mixed, an adequate quantity of silica sol (40wt. %) was gently introduced to the solution under rigorous stirring for 12h. Ultimately, 0.2% seed was added and hydrothermally processed in an oven at 180°C for 32 h [42].

2.3. Preparation of AgZSM-5

To gain the AgZSM-5 zeolite, the ion exchange route was utilized. In this matter, firstly, 5 g of the NaZSM-5 zeolite which was prepared in before was introduced to a 50 mL of a 1 M silver nitrate (AgNO_3) solution and this mixture was magnetically agitated at 60°C for 5 h. This agitation process

would be followed by an ion exchange by which Ag^+ ions were located instead of Na^+ ions. To eliminate the surplus Ag^+ ions from the zeolite framework, the resulted AgZSM-5 zeolite was consecutively filtered and washed by using the deionized water (D.W) and 0.1 M hydrochloric acid (HCl) solution prior to be dried at 110°C for 16 h. The cleaned and dried AgZSM-5 zeolite powder was then calcined at 400°C for 4 h. The demonstrated procedure was renewed thrice to approach sufficient ion exchange.

2.4. Preparation of CuO NPs/AgZSM-5

The CuO NPs/AgZSM-5 zeolite composite was prepared by the impregnation method. In a typical experimental procedure, 4 g of the AgZSM-5 zeolite was introduced to a solution of 2 M of copper nitrate trihydrate ($\text{Cu}(\text{NO}_3)_2 \cdot 3\text{H}_2\text{O}$) reactant in 150 mL deionized water (D.W). After that, the mixture was rigorously stirred at room temperature for 6h. After accomplishment of the reaction, the obtained sample were filtered, washed by the deionized water (D.W) several times and dried nightlong at 110°C before the next process. The acquired product was specified after calcination at 500°C and being settled in air for 6h. Furthermore, the raw CuO NPs was also synthesized in the absence of the AgZSM-5 zeolite under equal conditions.

2.5. Removal reaction tests of 2-CEPS over CuO NPs/AgZSM-5

The removal (adsorption and degradation) reaction of 2-chloroethyl phenyl sulfide (2-CEPS) sulfur mustard agent simulate on the CuO NPs/AgZSM-5 composite is comprehended according to the following approach. In a typical manner, 10 mL of n-decane as the solvent, 200 μL of n-octane as the internal standard, and 25, 50, 75 and 100 mg/L of 2-CEPS were introduced to a 50 mL Erlenmeyer flask which was toughly sealed to resist the solvent vaporization. More, the resulting samples were all sufficiently stirred for 2 min to attain homogeneous mixture. Afterwards, the amounts of 0.1, 0.2, 0.3, 0.4, 0.5, and 0.6 g of CuO NPs/AgZSM-5 composite were added to the above prepared solutions, respectively. Further, no attempt was implemented to control surrounding ambient conditions for instance humidity or light. Afterwards, all of the supplied samples were gently shaken for 15, 30, 45, 60, 75, 90, 115 and 120 min on a wrist-action shaker to attain a noticeable adsorption and a substantial interaction between the CuO NPs/AgZSM-5 composite and 2-CEPS. These obtained solution samples were then left to be settled until the precipitation process was fully completed. Finally, 10 μL of upper solution of each sample was picked up via a micro-syringe and then injected to the GC-FID and GC-MS devices to get further quantitative view.

3. Results and discussion

3.1. SEM

The characteristics such as morphology and crystalline size of the synthesized parent NaZSM-5 zeolite, AgZSM-5 zeolite, CuO NPs/AgZSM-5 zeolite composite and plus raw CuO NPs were investigated via the Field emission scanning electron microscopy (FESEM) technique, and the related results represented in Fig.1. The SEM micrographs display uniformly morphology of the NaZSM-5 (Fig.1a) and AgZSM-5 (Fig.1b) zeolites as the hexagonal cubic and also quasi-spherical CuO NPs

which were desirably supported on the AgZSM-5 zeolite surface (Fig.1c). Besides, the SEM micrographs prove the assumption that Ag^+ ion exchange and CuO NPs loading processes had no sensible negative impact on the morphology and the crystallinity of the structures. The mediocre crystalline size of the synthesized AgZSM-5 zeolite and CuO NPs in the CuO NPs/AgZSM-5 composite framework was estimated to be 2 micron and less than 20 nm, respectively.

3.2. EDX

To investigate the elemental composition of the pre-prepared parent NaZSM-5 zeolite, CuO NPs/AgZSM-5 zeolite composite and raw CuO NPs, more study was implemented in detail by the energy dispersive X-rays (EDX) analysis technique and the affiliated outcome was collected in Fig.2. From Fig.2, it can be undoubtedly inferred that the Na, O, Al, and Si elements are present in the NaZSM-5 and CuO NPs/AgZSM-5 structures. In the provided EDX spectra, the emerged peaks in the ranges of nearly 0.5 to 2 are respectively attributed to the binding energies of O, Na, Al, and Si which are referred to the main elements of the ZSM-5 zeolite (Fig.2a). Moreover, in spectrum (Fig.2b), the two emerged peaks in the ranges of 2.92 and 3.21 keV are attributed to the binding energies of Ag and three observed peaks in the ranges of 0.93, 8.04 and 9.03 keV are corresponded to the binding energies of Cu. This confirms the existence of Cu in the synthesized composite. On the other hand, the obtained information also reveals the coexistence of 3.4 wt.% Ag and 12.6 wt.% CuO in the synthesized composite structure, respectively. As can be seen, the Fig.3 depicts an instance SEM image of the synthesized composite with the related EDX elemental mappings. The major concentration of the related element has been indicated by a brighter area in the elemental map. In this regard, each of the various elements has been depicted in different color in order to simplify the identification of their positions within the nanomaterials. As it has been represented in Fig.3, the related elemental dot-mappings clearly point the presence of O, Al, Si, Ag, and Cu. According to maps, the homogeneity of the sample can be proved by the uniform distribution of elements over the composite.

3.3. TEM

The shape and size of the pre-synthesized CuO NPs/AgZSM-5 zeolite composite (Fig.3a) and raw CuO NPs (Fig.3b) were meticulously surveyed by the transmission electron microscopy (TEM) as the corresponding images have been depicted in Fig.3. Besides, the high magnification TEM micrograph in Fig.3a displays the loaded dark particles of CuO NPs with mediocre particle size of 16 nm on the bright surface of AgZSM-5 zeolite. The gained results were in good consistency with the mediocre particle size calculated via the Debye-Scherrer formula from the XRD pattern.

3.4. XRD

Fig.4 comprises the typical powder X-ray diffraction (XRD) patterns of the parent NaZSM-5 zeolite, AgZSM-5 zeolite, CuO NPs/AgZSM-5 zeolite composite, and raw CuO NPs, respectively. As can be observed in the patterns, the six obvious main and narrow peaks relating to the NaZSM-5 zeolite emerged at 2θ of 7.1945° , 8.9836° , 14.4871° , 22.8369° , 23.1653° , and 46.5112° (Fig.4a) were

referred to the diffraction planes of (101), (200) (301), (511), (303), and (503), respectively and are in accordance with those of the NaZSM-5 zeolite with JCPDS Card No. 025-1349 which are marked with orange circle symbols. The NaZSM-5 zeolite framework was undergone no change even after Ag^+ ion exchange process which led to form the expected AgZSM-5 (Fig.4b). Meantime, the synthesized CuO NPs playing the role of guest material were loaded as a 12.6 wt.% onto the AgZSM-5 zeolite which was considered as the host material. This momentous phenomenon dictates a series of new appeared peaks gained at 2θ of 41.5541° , 45.3006° , and 57.2789° referring to the diffraction planes of (002), (111), and (202) respectively which are marked with black square symbols. Furthermore, there was no identified characteristic peak implying the impurities during the loading process of CuO species. Also, the particle size of the synthesized CuO NPs included on the AgZSM-5 was further explored by XRD technique and line broadening of the peak at $2\theta=4^\circ\text{-}80^\circ$ as measured by the Debye-Scherrer equation: $D_{XRD} = \frac{0.9\lambda}{\beta \cos \theta}$. In the noted equation, D_{XRD} is corresponded to the mediocre crystallite size, λ refers to the wavelength of CoK_α radiation, β is known as the full width at half maximum (FWHM) of the selected diffraction peak and θ is defined as the Bragg diffraction angle. The peaks related to the raw CuO NPs appeared at scattering angles $2\theta= 37.9235^\circ$, 41.5511° , 45.2733° , 57.2749° , 62.982° , 68.8817° , 72.9301° and 78.8443° affiliating to the diffraction planes of (100), (002), (111), (202), (113), (220), (311), and (222), respectively which crystallized in the monoclinic phase and were in good consistency with those of CuO NPs with the literature values (JCPDS Card No. 05-0661). From the above specified equation, the mediocre particle size for CuO NPs in the CuO NPs/AgZSM-5 zeolite composite is calculated 16.2 nm. The calculated particle size from XRD measurement is in good agreement with the attained results from the SEM analysis.

3.5. FTIR

The Fourier transform infrared (FTIR) was used to determine the functional groups and the typical bands of the parent NaZSM-5 zeolite, AgZSM-5 zeolite, CuO NPs/AgZSM-5 zeolite composite, raw CuO NPs, and 2-CEPS-CuO NPs/AgZSM-5 zeolite composite, and resulting are recorded in Fig.5. It is also notable that the peak positions are approximately the same for all four ZSM-5 zeolite samples. All these pre-synthesized particular samples, including NaZSM-5, AgZSM-5, and CuO NPs/AgZSM-5 show representative sharp peaks about 451 cm^{-1} and 545 cm^{-1} which are attributed to the bending vibrations of the insensitive internal SiO_4 or AlO_4 tetrahedral units and plus double five-member rings in the pentasil framework of ZSM-5(MFI) type zeolite, respectively. The peaks occurred about 796 cm^{-1} , 1093 cm^{-1} and 1224 cm^{-1} are assigned to the internal tetrahedral symmetrical and asymmetrical stretching vibrations of Si-O-Si linkages of the ZSM-5 zeolite framework, respectively. Besides, the peaks emerged about 1633 cm^{-1} and 3649 cm^{-1} can be referred to the H-O-H bending O-H bonding vibrations and physically adsorbed H_2O molecules of the ZSM-5, respectively. Delving into the Figs. 5a-5c verifies the assumption that no phenomenal variation has observed in the bands of AgZSM-5 zeolite and CuO NPs/AgZSM-5 zeolite composite compared with the parent NaZSM-5 zeolite. This

fact encourages the opinion that the ion exchange and loading procedures of NaZSM-5 zeolite by the Ag^+ ion and CuO shows a negligible effect on the chemical structure of the zeolite structure. Fig.5c displays a new occurred peak corresponding to the loaded CuO NPs. The absorption peak appeared at 929 cm^{-1} is attributed to Cu-O-Al and Cu-O-Si bonds which uncovers the trapped CuO in the zeolite framework structure. On the other hand, Fig.5e shows the FTIR spectrum of the raw synthesized CuO NPs. The broad absorption peaks observed around 3675 cm^{-1} and 1620 cm^{-1} are corresponded to the adsorbed H_2O molecules. Also, three recognized peaks at 482 cm^{-1} and 525 cm^{-1} are assigned to the stretching vibrations of Cu-O bonding. Besides, to provide much more intelligible demonstration about the adsorption process of 2-CEPS on the synthesized adsorbent composite, the FTIR analysis was applied after the reaction and the corresponding spectrum were precisely recorded. As can be observed in Fig.5d, two new substantial absorption peaks spotted at 1276 cm^{-1} and 1508 cm^{-1} are assigned to the S-C and C=C bonds, respectively.

3.6. Removal of 2-CEPS on the CuO NPs/AgZSM-5

3.6.1. Effect of contact time

The gas chromatograph-flame ionization detector (GC-FID) analysis was operated to study and monitor the performance of the synthesized CuO NPs/AgZSM-5 zeolite composite adsorbent for the removal (adsorption and degradation) of 2-CEPS in aqueous solution. To gain the highest reaction efficiency, the important factors like reaction time were surveyed by employing n-decane as the solvent, a 120 min time considered as the shaking time and also the temperature of 25°C , respectively. Figs.6 and 7 illustrate the so-called area under curve (AUC) data under above defined conditions of GC-FID chromatograms. From the GC-FID chromatograms it is brightly comprehended that 2-CEPS displays a retention time around 15.3 min. Further, to acquire the degradation quantity, the integrated AUC data of two samples of 2-CEPS and n-octane as the internal standard were computed for all variables and its ratio (integrated AUC of CEPS/integrated AUC of n-octane) was determined. Several time intervals were selected for various respective experiments to reach to the optimum time of reaction for the removal of 2-CEPS on the synthesized CuO NPs/AgZSM-5 composite. The mentioned experiments uncover the apparent relationship between removal characteristic of adsorbent and different time intervals. In this matter, Figs. 6-8 depict the changes in the removal (%) against stirring time and the obtained product% (2-HEPS%, with retention time about 17.9 min) at different initial 2-CEPS concentration and plus the correlation between removal efficiency of 2-CEPS on the synthesized CuO NPs/AgZSM-5 composite to the contact time. Therefore, the reaction time was surveyed in the scope of 0 to 120 min. To reach the most appropriate reaction time and subsequently the highest removal efficiency, 120 min was approved as an optimum value for the posterior sequential experiments. Additionally, in Fig.6, the GC-FID spectra and affiliated data have been shown.

3.6.2. Effect of adsorbent dose

Using the least amount of adsorbent to obtain the highest rate of removal is an undeniable key parameter that cannot be connived. It grants much more authenticity to the proposed method for further future development and investigations. In present research, to evaluate the best applicable quantity of adsorbent, a range of 0.1 to 0.6 g of the synthesized CuO NPs/AgZSM-5 adsorbent was applied for the removal of 2-CEPS. As has been represented in Fig.9, the increase in the adsorbent quantity is caused to higher degradation efficiency. Thenceforth, as this increase continued no substantial change recognized and the curve slope showed a linear behavior implying the constant values. Eventually, the value of 0.3 g of CuO NPs/AgZSM-5 adsorbent was denoted as the optimum value to conquer the high yield adsorption and subsequent degradation reaction.

3.6.3. Effect of adsorbent type

To compare the influence of adsorbent type on the removal efficiency, NaZSM-5 zeolite, AgZSM-5 zeolite, CuO NPs/AgZSM-5 zeolite composite and raw CuO NPs were prepared as four segregated adsorbents for the adsorption and degradation process of 2-CEPS molecule. These series of experiments were designed and fulfilled under the similar conditions for the assigned adsorbents. Raw NaZSM-5 zeolite does not have high catalytic performance and that is why the loading process by Ag^+ and CuO NPs was applied to increase the catalytic role, respectively. It is also acknowledged that the raw CuO NPs represent the lower adsorption-degradation for 2-CEPS compared with NaZSM-5. Based on the Fig.10, it can be vividly deduced that the highest rate of adsorption and degradation of 2-CEPS observed for the CuO NPs/AgZSM-5 composite adsorbent which demonstrates the efficacious combination of CuO NPs with AgZSM-5 zeolite.

3.6.4. Reaction kinetics

As can be seen in Fig.11, the removal kinetics was investigated employing the plots of Ln concentration versus reaction time. The parameter k which is defined as the removal rate constant or in other word "slope", was calculated from the first order equation as follows: $\text{Ln } C_0/C_t = kt$. In this equation, parameter C_t is specified as the concentration of the 2-CEPS at time t, parameter C_0 is corresponded to the initial concentration and k is referred to the removal rate constant. Furthermore, the half-life ($t_{1/2}$) can be computed by $t_{1/2} = 0.693/k$. Also, 0.3 g of CuO NPs/AgZSM-5 composite was introduced into the discrete containers including 25 mg/L of 2-CEPS at definite time intervals to study the reaction kinetics. The respective results have been represented in Table 1.

3.6.5. GC-MS

The compound originated from the degradation and hydrolysis of 2-CEPS on the CuO NPs/AgZSM-5 composite adsorbent was identified by gas chromatography coupled with mass spectrometry (GC-MS) analysis. Fig.12 exhibits four significant peaks at various retention times. The peaks about 9.5 and 10.5 min are assigned to the n-octane internal standard and n-decane solvent, respectively. Besides, two other sharp peaks about 15.3 and 17.9 min are identified which is attributed to the 2-CEPS and its degraded product namely 2-HEPS, respectively. Further, the detector was programmed to scan a mass

range of 28, 45, 65, 77, 91, 109, 123 and 172 m/z (Fig.12a), and 28, 45, 59, 77, 85, 131 and 154 m/z (Fig.12b) for 2-CEPS, and 2-HEPS, respectively.

3.6.6. Mechanism of the 2-CEPS removal

According to the provided information from GC-FID and GC-MS analyses, the proposed mechanism schemes for the adsorption and degradation (removal) procedure of the 2-CEPS on the CuO NPs/AgZSM-5 composite adsorbent and beside the formation of degradation product have been shown in (Scheme 1a and 1b). In the assigned scheme, the role of both silver (Ag^+) and copper oxide (CuO) species on the removal reactions have been separately reviewed. It should be also assumed that both of the represented routes are conceivable and may proceed simultaneously. In route (Scheme 1a) first, the Cl atom of 2-CEPS molecule undergoes a nucleophilic attack by the Bronsted acid sites (hydroxyl groups (Cu-OH)) which are present through the CuO of the CuO NPs/AgZSM-5 composite structure. During this phenomenon, an intermediate of cyclic sulfonium ion is expected to be formed but it is the nonvolatile form of the corresponding compound so that its extraction and subsequent detection by the GC-FID is not possible. Then after a short interval, de-halogenation reaction causes the elimination of the chlorine atom from 2-CEPS molecule. Meanwhile, whether the H_2O molecule is present or not, various reactions are probable to proceed and hydrolysis originated substance will be revealed on the surface of Cu species (Cu^{2+}) as the Lewis acid sites. The hydrolysis process goes on until 2-hydroxyl ethyl phenyl sulfide (2-HEPS) as the major removal product of 2-CEPS is emerged. In contrast, in route (Scheme 1b) the chlorine and sulfur atoms of sulfur mustard agent simulate undergo an electrophilic attack by positive silver (Ag^+) from the zeolite structure and as a results forces 2-CEPS molecule to be adsorbed on the surface and pores of the composite. The transition states for the creation of S- Ag^+ -Cl bonds will also lead to form cyclic sulfonium ion which is recognized as an intermediate. These impermanent intermediates, in the presence of H_2O , change into 2-hydroxyl ethyl phenyl sulfide (2-HEPS) which is known as the hydrolysis product on the surface of silver species (Ag^+) as the Lewis acid sites of the synthesized CuO NPs/AgZSM-5 composite.

4. Conclusion

In the current research, the synthesis and application of CuO NPs/AgZSM-5 zeolite composite as a novel adsorbent for the adsorption and degradation of 2-chloroethyl phenyl sulfide (2-CEPS, a sulfur mustard agent simulate) was evaluated via the GC-FID analysis. Furthermore, the effect of several operative variables such as contact time, initial concentration, adsorbent dose and adsorbent type on the removal efficiency were meticulously surveyed and discussed. Afterwards the significant structural, morphological and crystalline size of the CuO NPs/AgZSM-5 composite synthesized by the impregnation method was proved via different characterization studies. Considering the GC-FID analysis results, it can be clearly inferred that the 2-CEPS was significantly removed by the synthesized composite adsorbent with 100% yield under defined optimized conditions namely: contact time (120 min), initial concentration (25 mg/L), and adsorbent dose (0.3 g). The reaction kinetic study was also exerted by using the first order model and the related quantity of the half-life

($t_{1/2}$) and rate constant (k) were measured as 26.25 min and 0.0264 min^{-1} , respectively. Besides, the obtained characterizations information confirmed the substantial, applicability and particular potential of the synthesized adsorbent for high yield adsorption and degradation of 2-CEPS. Consequently, 2-hydroxy ethyl phenyl sulfide (2-HEPS) as the less-toxic degradation and hydrolysis product of 2-CEPS on the CuO NPs/AgZSM-5 composite adsorbent was detected and verified.

Acknowledgments

The authors give their sincere thanks to the Payame Noor University, Ramsar, Iran for all sincere supports.

References

- [1] A.P. Watson, D.M. Opresko, R.A. Young, V. Hauschild, Development and application of acute exposure guideline levels (AEGs) for chemical warfare nerve and sulfur mustard agents, *J. Toxicol. Environ. Health B.* 9 (2006) 173-263. doi: 10.1080/15287390500194441.
- [2] R. Vijayaraghavan, A. Kulkarni, S.C. Pant, P. Kumar, P.V.L. Rao, NGupta, A. Gautam, K. Ganesan, Differential toxicity of sulfur mustard administered through percutaneous, subcutaneous, and oral routes, *Toxicol. Appl. Pharmacol.* 202 (2005) 180-188. doi: 10.1016/j.taap.2004.06.020.
- [3] N. Sharma, R. Kakkar, Recent advancements on warfare agents/metal oxides surface chemistry and their simulation study, *Adv. Mat. Lett.* 4 (2013) 508-521. doi: 10.5185/amlett.2012.12493.
- [4] M. Sadeghi, M.H. Hosseini, Preparation and application of MnO₂ nanoparticles/zeolite AgY composite catalyst by confined space synthesis (CSS) method for the desulfurization and elimination of SP and OPP, *J Nanostruct.* 2 (20 13) 441-455.
- [5] M. Sadeghi, M. Hosseini, Nucleophilic chemistry of the synthesized magnesium oxide(magnesia) nanoparticles via microwave@sol-gel process for removal of sulfurous pollutant, *Int. J. Bio-Inorg. Hybd. Nanomat.* 1 (2012) 175-182.
- [6] A. Mehrizad, P. Gharbani, Study on catalytic and photocatalytic decontamination of (2-chloroethyl) phenyl sulfide with nano-TiO₂, *Int. J. Nanosci. Nanotechnol.* 7 (2011) 48-53.
- [7] R.J. Argauer, G.R. Landolt, US Patent 3,702,886 (1972).
- [8] N. Kumar, V. Nieminen, K. Demirkan, T. Salmi, D.Y. Murzin, E. Laine, Effect of synthesis time and mode of stirring on physico-chemical and catalytic properties of ZSM-5 zeolite catalysts *Appl. Catal. A: Gen.* 235 (2002) 113-123. doi: 10.1016/S0926-860X(02)00258-2.
- [9] C. Falamaki, M. Edrissi, M. Sohrabi, Studies on the crystallization kinetics of zeolite ZSM-5 with 1,6-hexanediol as a structure-directing agent, *Zeolites*, 19 (1997) 2-5. doi: 10.1016/S0144-2449(97)00025-0.
- [10] Y.Ni, A. Sun, X. Wu, G. Hai, J. Hu, T. Li, G. Li, The preparation of nano-sized H[Zn, Al]ZSM-5 zeolite and its application in the aromatization of methanol, *Microporous Mesoporous Mater.* 143 (2011) 435-442. doi:10.1016/j.micromeso.2011.03.029.

- [11] S. Sang, F. Chang, Z. Liu, C. He, Y. He, L. Xu, Difference of ZSM-5 zeolites synthesized with various templates, *Catal. Today* 93–95 (2004) 729-734. doi: 10.1016/j.cattod.2004.06.091.
- [12] S.S. Kim, J. Shah, T. J. Pinnavaia, Colloid-imprinted carbons as templates for the nanocasting synthesis of mesoporous ZSM-5 Zeolite, *Chem. Mater.* 15 (2003) 1664-1668. doi: 10.1021/cm021762r.
- [13] O. Raymond, H. Villavicencio, V. Petranovskii, J.M. Sequeiros, Growth and characterization of ZnS and ZnCdS nanoclusters in mordenite zeolite host, *Mater. Sci. Eng. A.* 360 (2003) 202-206. doi: 10.1016/S0921-5093(03)00463-5.
- [14] M. Sathish, B. Viswanathan, R.P. Viswanath, Alternate synthetic strategy for the preparation of CdS nanoparticles and its exploitation for water splitting, *Int. J. Hydrogen Energy.* 31 (2006) 891-898. doi: 10.1016/j.ijhydene.2005.08.002.
- [15] X. Wang, Y. Guo, L. Yang, M. Han, J. Zhao, Nanomaterials as sorbents to remove heavy metal ions in wastewater treatment. *J. Environ. Anal. Toxicol.* 2 (2012) 154. doi:10.4172/2161-0525.1000154.
- [16] A. Mattsson, C. Lejon, V. Štengl, S. Bakardjieva, F. Opluštil, P.O. Andersson, L. Österlund, Photodegradation of DMMP and CEES on zirconium doped titania nanoparticles, *Appl. Catal. B: Environ.* 92 (2009) 401-410. doi: 10.1016/j.apcatb.2009.08.020.
- [17] D.A. Panayotov, J. R. Morris, Thermal decomposition of a chemical warfare agent simulant (DMMP) on TiO₂: adsorbate reactions with lattice oxygen as studied by infrared spectroscopy, *J. Phys. Chem. C* 113 (2009) 15684-15691. doi: 10.1021/jp9036233.
- [18] S.P. Decker, J.S. Klabunde, A. Khaleel, K. J. Klabunde, Catalyzed destructive adsorption of environmental toxins with nanocrystalline metal oxides. fluoro-, chloro-, bromocarbons, sulfur, and organophosphorus compounds, *Environ. Sci. Technol.* 36 (2002) 762-768. doi: 10.1021/es010733z.
- [19] W. O. Gordon, B.M. Tissue, J.R. Morris, Adsorption and decomposition of dimethyl methylphosphonate on Y₂O₃ nanoparticles, *J. Phys. Chem. C* 111 (2007) 3233-3240. doi: 10.1021/jp0650376.
- [20] Y.X. Li, O. Koper, M. Attaya, K. Klabunde, Adsorption and decomposition of organophosphorus compounds on nanoscale metal oxide particles. In situ GC-MS studies of pulsed microreactions over magnesium oxide, *J. Chem. Mater.* 4 (1992) 323-330. doi: 10.1021/cm00020a019.
- [21] M.A. Sayyadnejad, H.R. Ghaffarian, M. Saeidi, Removal of hydrogen sulfide by zinc oxide nanoparticles in drilling fluid, *Int. J. Environ. Sci. Technol.* 5 (2008) 565-569.
- [22] S. Yekta, M. Sadeghi, E. Babanezhad, N. Shahabfar, Preparation of sodium dodecyl sulfate modified pyrrolidine-1-dithiocarboxylic acid ammonium coated magnetite nanoparticles for magnetic solid phase extraction of Pb(II) from water samples, *Int. J. Bio-Inorg. Hybr. Nanomater.* 3 (2014) 143-156.
- [23] S. Srivastava, M. kumar, A. Agrawal, S. Kumar Dwivedi, Synthesis and characterisation of copper oxide nanoparticles, *J. Appl. Phys.* 5 (2013) 61-65.

- [24] D. Wu, Q. Zhang, M. Tao, LSDA+U study of cupric oxide: Electronic structure and native point defects, *Phys. Rev. B*: 73 (2006) 235206. doi: 10.1103/PhysRevB.73.235206.
- [25] A. Vyacheslav, I.E. Moshnikov, V.V. Gracheva, A.I. Kuznezov, S. Maximov, S.Karpova, A. A.Ponomareva, Hierarchical nanostructured semiconductor porous materials for gas sensors, *J. Non. Cryst. Solids*. 356 (2010) 2020-2025. doi: 10.1016/j.jnoncrsol.2010.06.030.
- [26] T.Yu-Feng, H. Shu-Jun, Y. Shi-Shen, M.Liang-Mo, Oxide magnetic semiconductors: Materials, properties, and devices, *Chin. Phys. B* 22 (2013) 088505. doi: 10.1088/1674-1056/22/8/088505.
- [27] P. Poizot, S. Laruelle, S.Grugeon, L.Dupontl, J.M. Tarascon, Nano-sized transition-metal oxides as negative-electrode materials for lithium-ion batteries, *Nature* 496 (2000) 496-499. doi:10.1038/35035045.
- [28] T. Hirano, S. Kanemaru, J. Itoh, A new metal-oxide-semiconductor field-effect-transistor-structured si field emitter tip, *Jpn. J. Appl. Phys.* 35 (1996) 861. doi: 10.1143/JJAP.35.L861.
- [29] J. Wensel, B. Wright, D. Thomas, W. Douglas, B. Mannhalter, W. Cross, H. Hong, J. Kellar, Enhanced thermal conductivity by aggregation in heat transfer nanofluids containing metal oxide nanoparticles and carbon nanotubes, *Appl. Phys. Lett.* 92 (2008) 023110. doi:10.1063/1.2834370.
- [30] M.K. Wu, J.R. Ashburn, C.J. Torng, P.H. Hor, R.L. Meng, L. Gao, Superconductivity at 93 K in a new mixed-phase Y-Ba-Cu-O compound system at ambient pressure, *Phys. Rev. Lett.* 58 (1987) 908. doi:10.1103/PhysRevLett.58.908.
- [31] J. Cao, G. Song Shao, Y. Wang, Y. Liu, Z.Y. Yuan, CuO catalysts supported on attapulgite clay for low-temperature CO oxidation, *Catal. Commun.* 9 (2008) 2555-2559. doi: 10.1016/j.catcom.2008.07.016.
- [32] T.H. Mahato, B. Singh, A.K. Srivastava, G.K. Prasad, A.R. Srivastava, K. Ganesan, R. Vijayaraghavan, Effect of calcinations temperature of CuO nanoparticle on the kinetics of decontamination and decontamination products of sulphur mustard, *J. Hazard. Mater.* 192 (2011) 1890-1895. doi: 10.1016/j.jhazmat.2011.06.078.
- [33] M. Verma, V.K. Gupta, V. Dave, R. Chandra, G.K. Prasad, Synthesis of sputter deposited CuO nanoparticles and their use for decontamination of 2-chloroethyl ethyl sulfide (CEES), *J. Colloid Interface Sci.* 438 (2015) 102–109. doi: 10.1016/j.jcis.2014.09.060.
- [34] P. Mallick, S. Sahu, Structure, microstructure and optical absorption analysis of CuO nanoparticles synthesized by sol-gel route, *J. Nanosci. Nanotechnol.* 2 (2012) 71-74. doi: 10.5923/j.nn.20120203.05.
- [35] K. Phiwdang, S. Suphankij, W. Mekprasart, W. Pecharapa, Synthesis of CuO nanoparticles by precipitation method using different precursors, *Energy procedia.* 34 (2013) 740–745. doi: 10.1016/j.egypro.2013.06.808.
- [36] M.S. Niasari, F. Davar, Synthesis of copper and copper(I) oxide nanoparticles by thermal decomposition of a new precursor, *Mater. Lett.* 63 (2009) 441-443. doi: 10.1016/j.matlet.2008.11.023.

- [37] A. El-Trass, H. ElShamy, I. El-Mehasseb, M. El-Kemary, CuO nanoparticles: synthesis, characterization, optical properties and interaction with amino acids, *Appl. Surf. Sci.* 258(2012) 2997-3001. doi: 10.1016/j.apsusc.2011.11.025.
- [38] P. Sanpui , A. Murugadoss , P.V. Durga Prasad , S. Sankar Ghosh , A. Chattopadhyay, The antibacterial properties of a novel chitosan-Ag-nanoparticle composite, *Int. J. Food Microbiol.* 124 (2008) 142-146. doi: 10.1016/j.ijfoodmicro.2008.03.004.
- [39] S.Q Sun, B Sun, W. Zhang, D Wang, Preparation and antibacterial activity of Ag-TiO₂ composite film by liquid phase deposition (LPD) method, *Bull. Mater. Sci.* 31 (2008) 61-66.
- [40] M. Sadeghi, S. Yekta, H. Ghaedi, Synthesis and application of Pb-MCM-41/ZnNiO₂ as a novel mesoporous nanocomposite adsorbent for the decontamination of chloroethyl phenyl sulfide (CEPS), *Appl. Surf. Sci.* 400 (2017) 471-480. doi: 10.1016/j.apsusc.2016.12.224.
- [41] M. Sadeghi, H. Ghaedi, S.Yekta, E. Babanezhad, Decontamination of toxic chemical warfare sulfur mustard and nerve agent simulants by NiO NPs/Ag-clinoptilolite zeolite composite adsorbent, *J. Environ. Chem. Eng.* 4 (2016) 2990-3000. doi: 10.1016/j.jece.2016.06.008.
- [42] M. Khatamiana, B. Divband, M. Daryana, Preparation, characterization and antimicrobial property of Ag⁺-nano chitosan/ZSM-5: novel hybrid biocomposites, *Nanomed. J.* 3 (2016) 268-279. doi: 10.22038/nmj.2016.7616.

Table1. First order kinetic parameters for the removal of 2-CEPS over CuO NPs/AgZSM-5 at different initial concentration.

Initial concentration (mg/L)	Half-life ($t_{1/2}$, min)	Rate constant (k , min^{-1})	First order kinetic equation
25	26.25	0.0264	$\text{Ln } C_0/C_t = 0.0264t - 0.1135$
50	55.44	0.0125	$\text{Ln } C_0/C_t = 0.0125t - 0.0045$
75	108.28	0.0064	$\text{Ln } C_0/C_t = 0.0064t + 0.0477$
100	150.65	0.0046	$\text{Ln } C_0/C_t = 0.0046t + 0.0463$

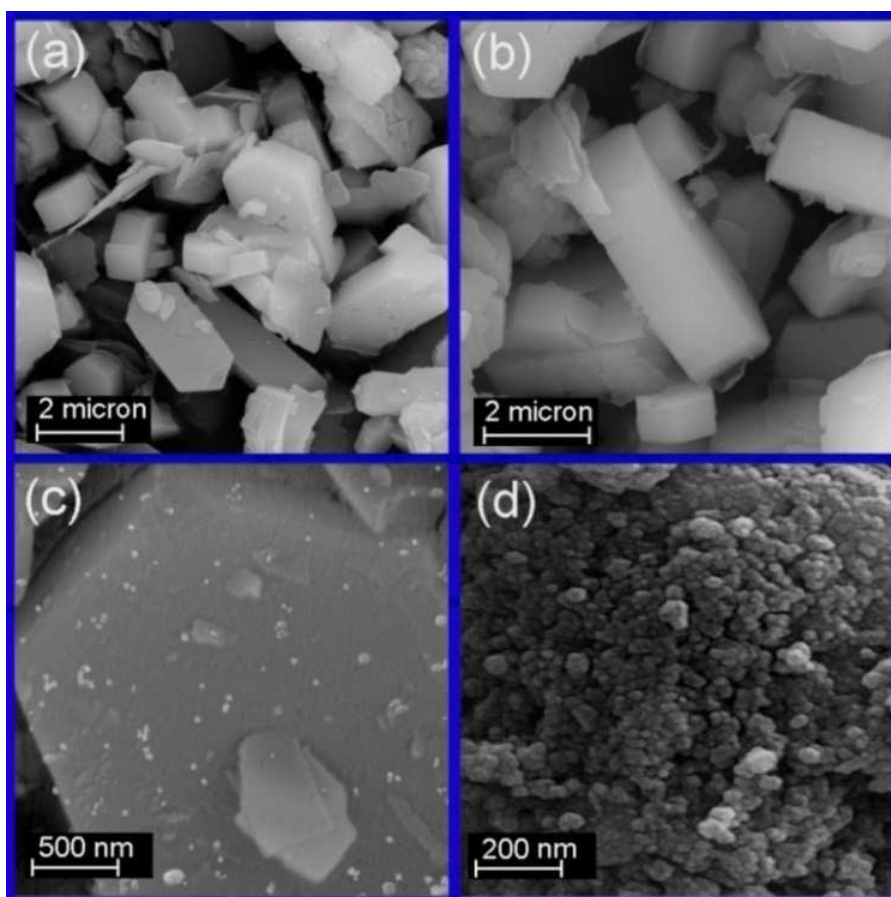


Fig.1. SEM micrographs of: a) parent NaZSM-5, b) AgZSM-5, c) CuO NPs/AgZSM-5, and d) raw CuO NPs.

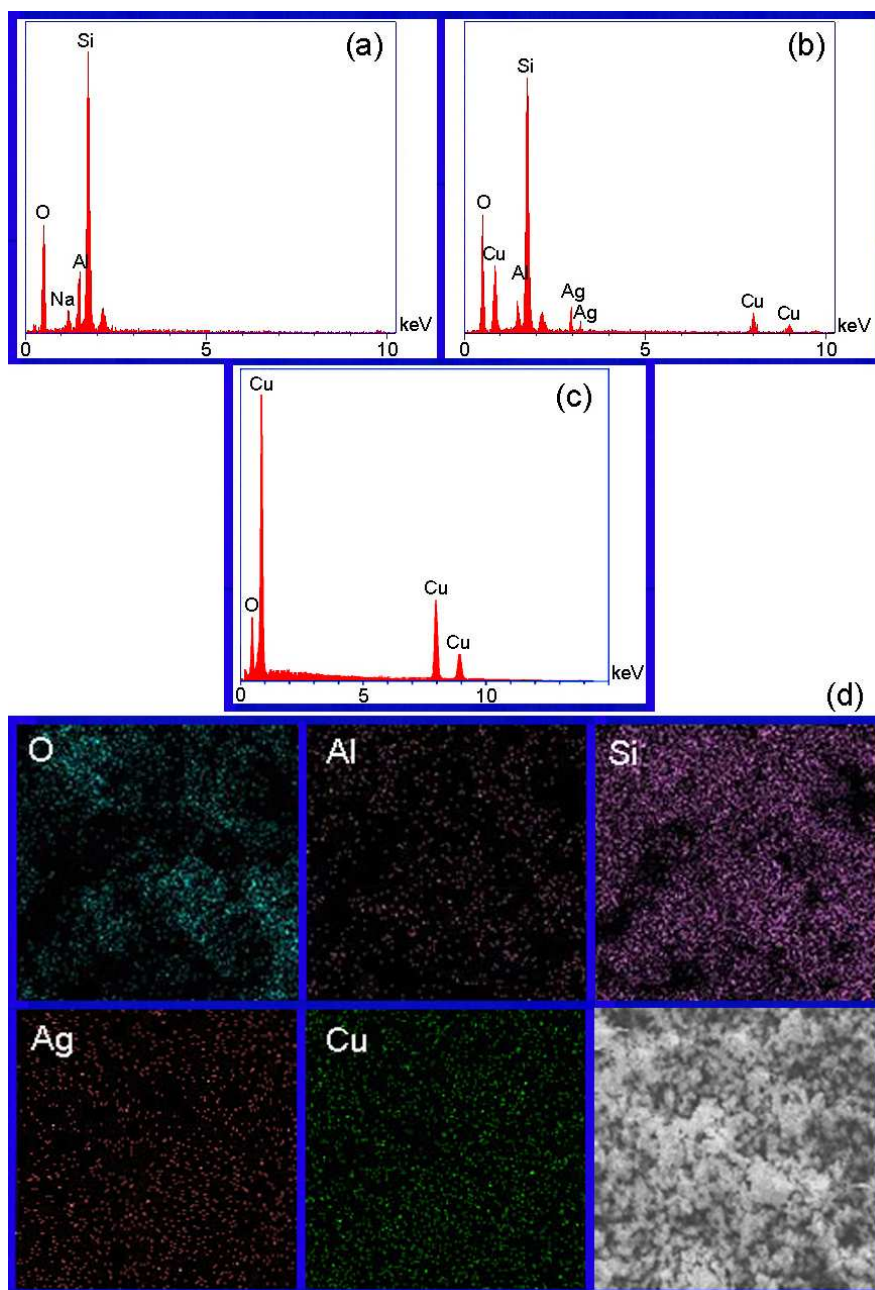


Fig.2. EDX analyses of: a) parent NaZSM-5, b) CuO NPs/AgZSM-5, c) raw CuO NPs, and d) SEM micrograph of the CuO NPs/AgZSM-5 with relating EDX dot-mappings which specifies the positions of various elements over the composite framework.

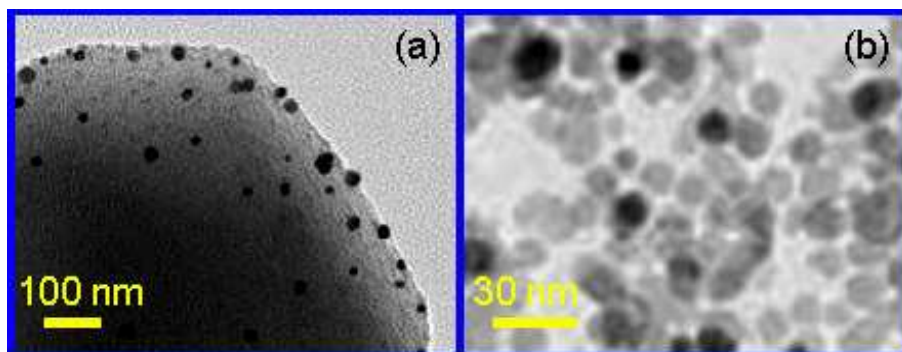


Fig.3. TEM micrographs of: a) CuO NPs/AgZSM-5, and b) raw CuO NPs.

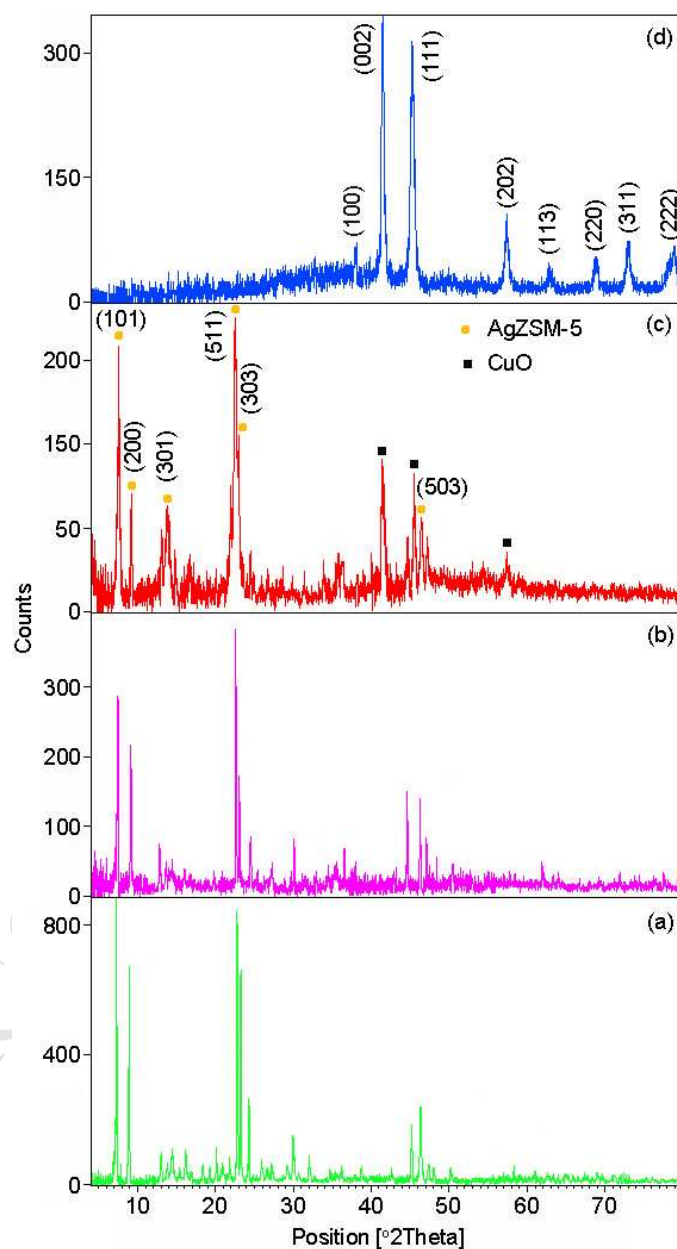


Fig.4. XRD patterns of: a) parent NaZSM-5, b) AgZSM-5, c) CuO NPs/AgZSM-5, and d) raw CuO NPs.

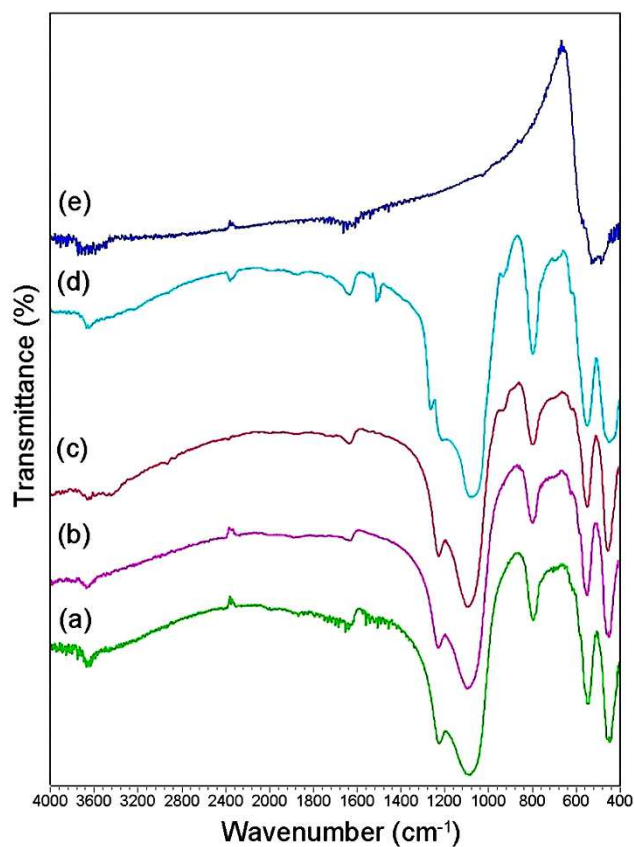


Fig.5. FTIR spectra of: a) parent NaZSM-5, b) AgZSM-5, c) CuO NPs/AgZSM-5, d) CuO NPs/AgZSM-5 after adsorption of 2-CEPS, and e) raw CuO NPs.

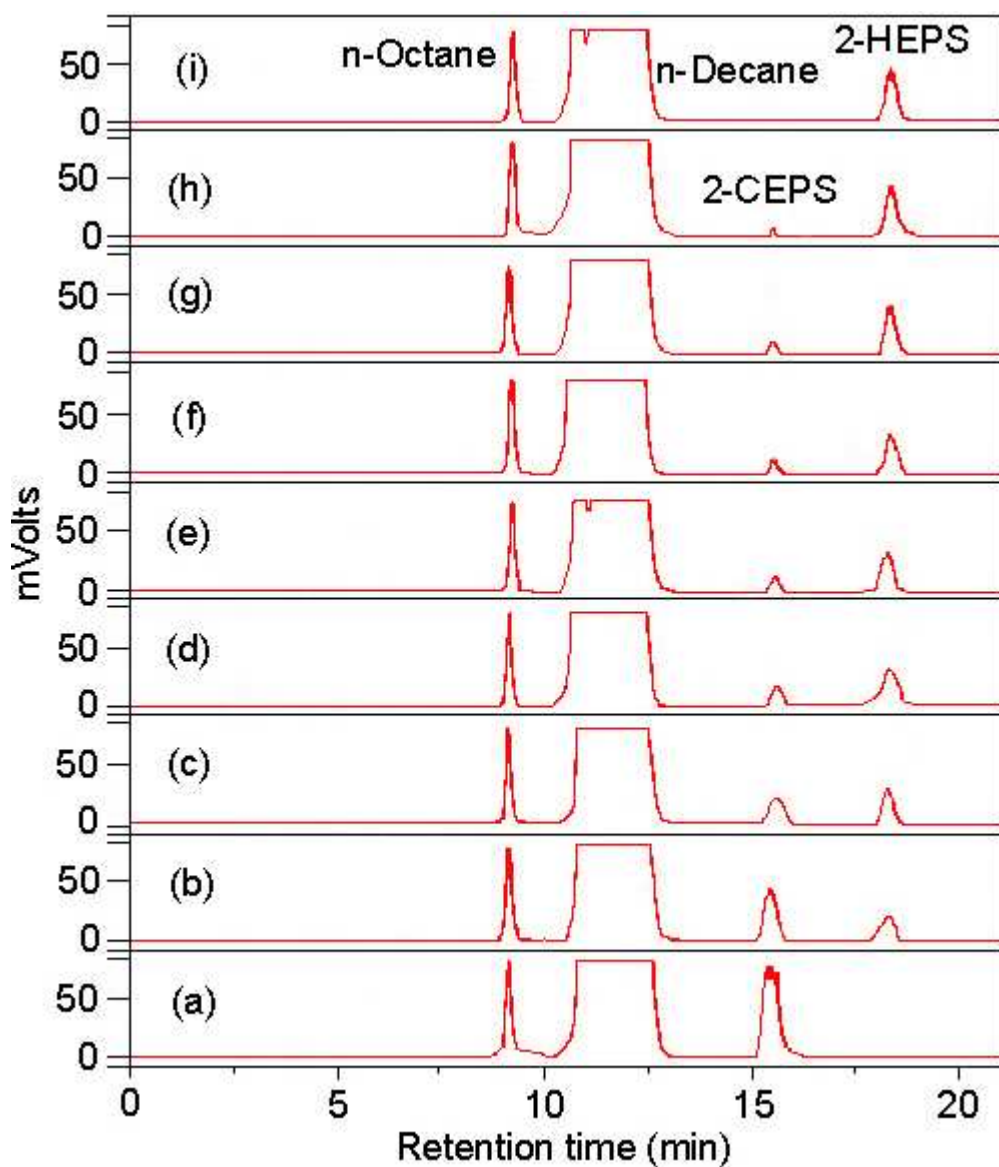


Fig.6. GC-FID chromatograms for the 2-CEPS-CuO NPs/AgZSM-5 sample at different contact times: a) 0, b) 15, c) 30, d) 45, e) 60, f) 75, g) 90, h) 115, and i) 120 min.

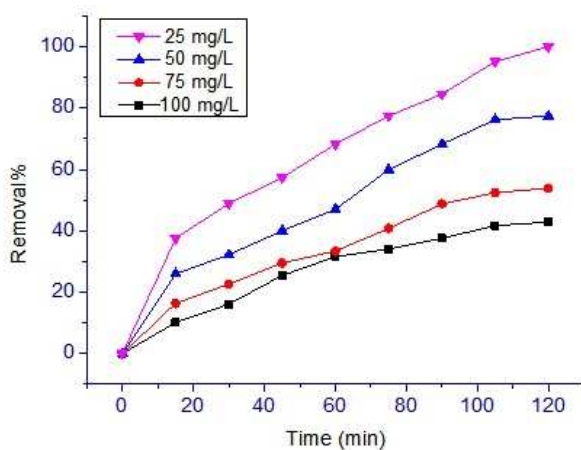


Fig.7. Effect of contact time on the removal of 2-CEPS over CuO NPs/AgZSM-5 at different initial concentrations.

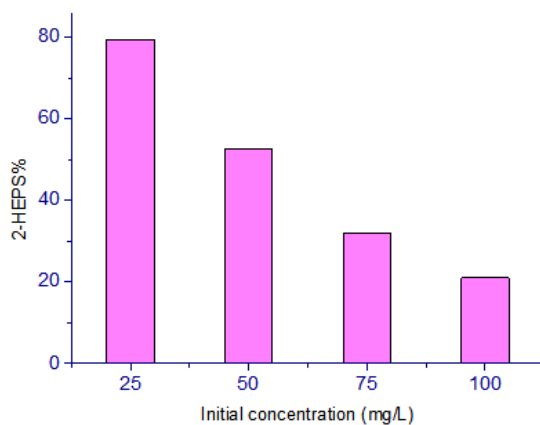


Fig.8. Plot of the obtained 2-HEPS% against initial concentration on the removal of 2-CEPS over CuO NPs/AgZSM-5 (optimum conditions: adsorbent dose: 0.3 g, and contact time: 120 min).

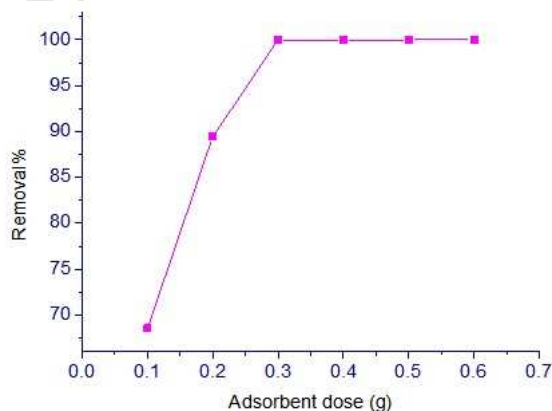


Fig.9. Effect of adsorbent dose on the removal of 2-CEPS over CuO NPs/AgZSM-5 (optimum conditions: initial concentration: 25 mg/L, and contact time: 120 min).

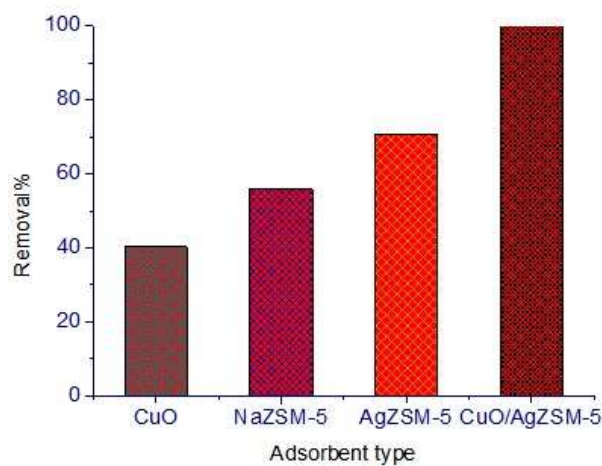


Fig.10. Effect of adsorbent type on the removal of 2-CEPS (optimum conditions: initial concentration: 25 mg/L, contact time: 120 min, and adsorbent dose: 0.3 g).

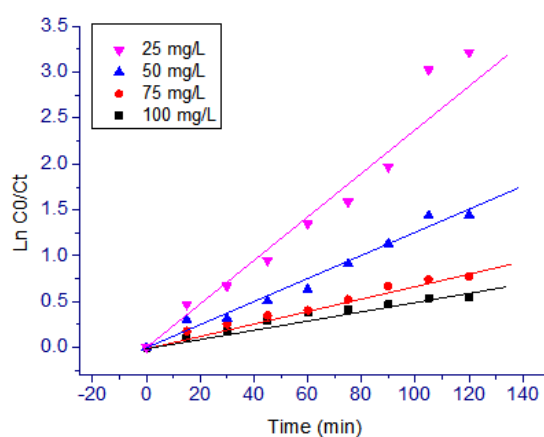


Fig.11. Plot of $\ln C_0/C_t$ against contact time on the removal of 2-CEPS over CuO NPs/AgZSM-5 composite at different initial concentrations.

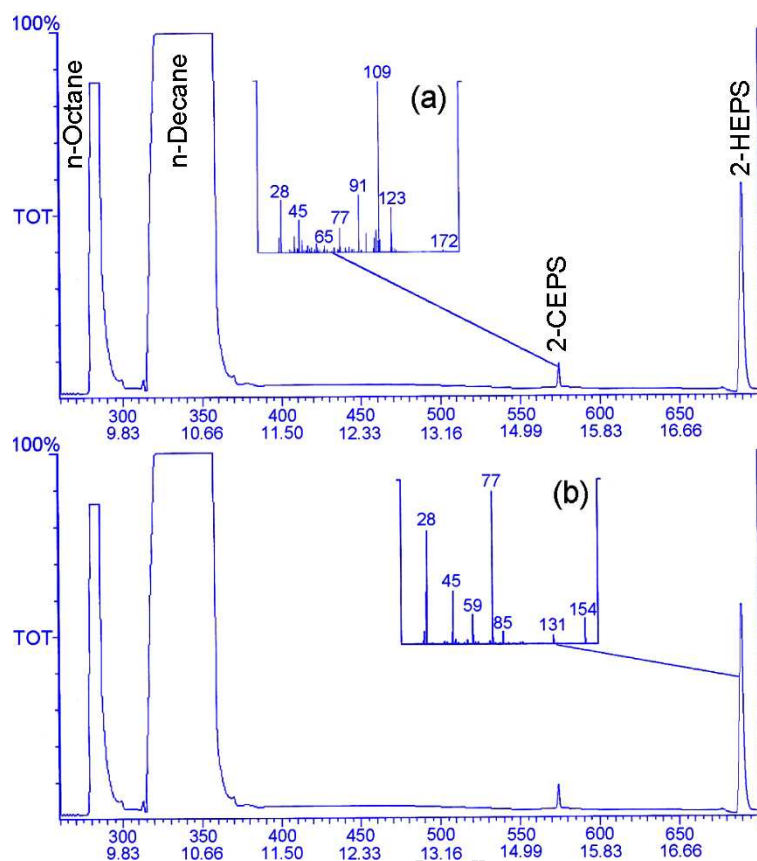
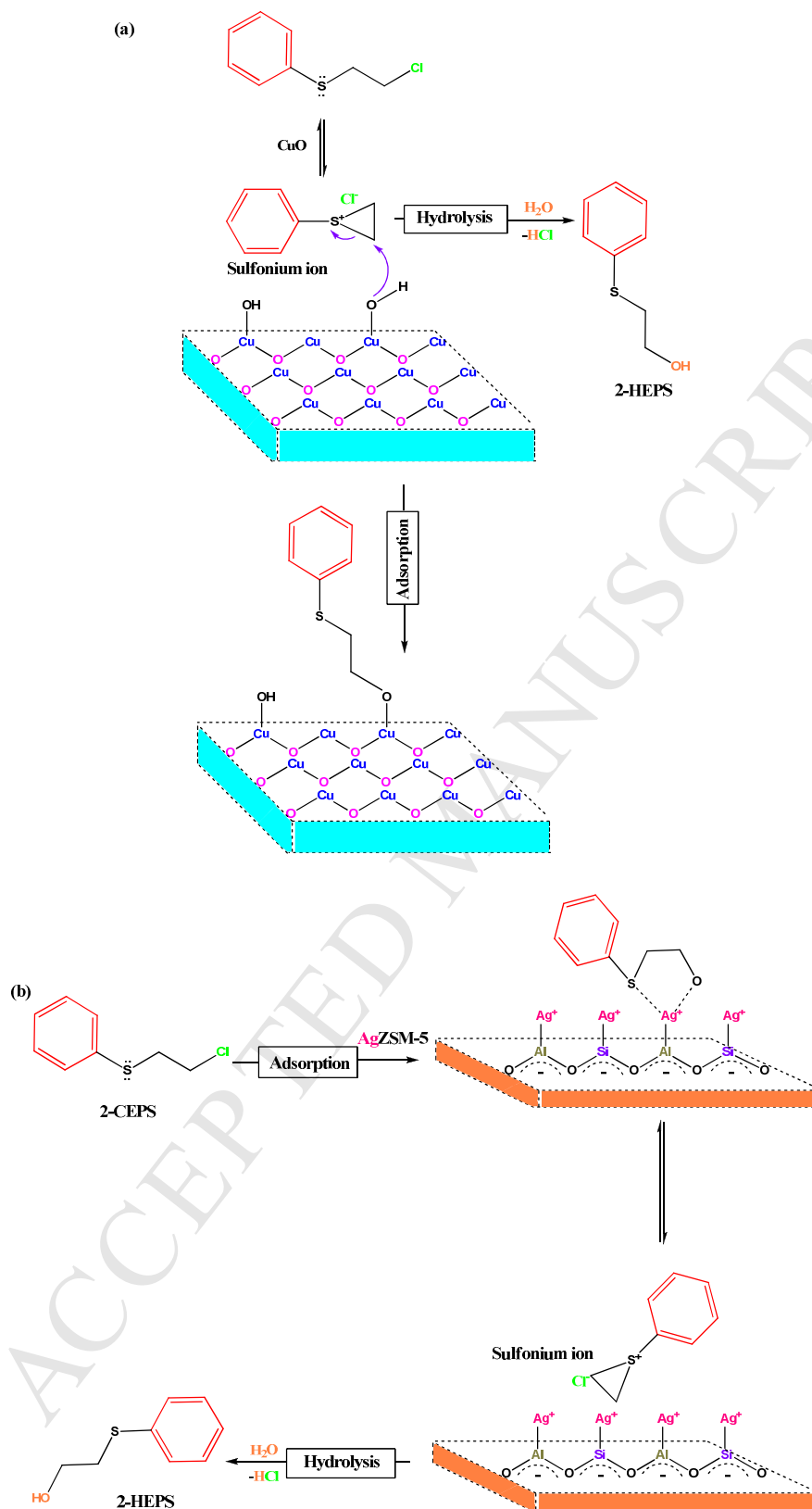


Fig.12. GC-MS analysis and mass spectra of the degradation and hydrolysis product of the CuO NPs/AgZSM-5 composite reaction with 2-CEPS: a) 2-CEPS, and b) 2-HEPS.



Scheme 1. Reaction mechanisms for the removal of 2-CEPS over CuO NPs/AgZSM-5.

Highlights:

- The CuO NPs/AgZSM-5 adsorbent composite was synthesized via the impregnation method.
- The CuO NPs/AgZSM-5 was applied for the high yield removal of 2-CEPS.
- The reaction kinetic status was also studied employing first order model.
- 2-hydroxy ethyl phenyl sulfide (2-HEPS) as the degradation product was attained.